Acta Geologica Sinica (English Edition), 2020, 94(1): 90–102

Genesis for Rare Earth Elements Enrichment in the Permian Manganese Deposits in Zunyi, Guizhou Province, SW China

XU Hai[1, 2], GAO Junbo[1, 2, *], YANG Ruidong[1, 2], DU Lijuan[1, 2], LIU Zhichen[3], CHEN Jun[4], FENG Kangning[1, 2] and YANG Guanghai[1, 2]

[1] *College of Resources and Environmental Engineering, Guizhou University, Guiyang 550025, China*
[2] *Key Laboratory of Karst Georesources and Environment, Ministry of Education, Guizhou University, Guiyang 550025, China*
[3] *102 Geological Team, Guizhou Bureau of Exploration and Development of Geology Mineral Resources, Zunyi, Guizhou 563003, China*
[4] *Institute of Geochemistry, Chinese Academy of Sciences, Guiyang 550081, China*

Abstract: The Zunyi manganese deposits, which formed during the Middle to Late Permian period and are located in northern Guizhou and adjacent areas, are the core area of a series of large-medium scale manganese enrichment minerogenesis in the southern margin and interior of the Yangtze platform, Southern China. This study reports the universal enrichment of rare earth elements (REEs) in Zunyi manganese deposits and examines the enrichment characteristics, metallogenic environment and genesis of REEs. The manganese ore bodies present stratiform or stratoid in shape, hosted in the silicon–mud–limestones of the Late Permian Maokou Formation. The manganese ores generally present lamellar, massive, banded and brecciated structures, and mainly consist of rhodochrosite, ropperite, tetalite, capillitite, as well as contains paragenetic gangue minerals including pyrite, chalcopyrite, rutile, barite, tuffaceous clay rock, etc. The manganese ores have higher ΣREE contents range from 158 to 1138.9 ppm (average 509.54 ppm). In addition, the ΣREE contents of tuffaceous clay rock in ore beds vary from 1032.2 to 1824.5 ppm (average 1396.42 ppm). The REEs from manganese deposits are characterized by La, Ce, Nd and Y enriched, and existing in the form of independent minerals (e.g., monazite and xenotime), indicating Zunyi manganese deposits enriched in light rare earth elements (LREE). The Ce_{anom} ratios (average −0.13) and lithofacies and paleogeography characteristics indicate that Zunyi manganese deposits were formed in a weak oxidation-reduction environment. The $(La/Yb)_{ch}$, Y/Ho, $(La/Nd)_N$, $(Dy/Yb)_N$, Ce/Ce^* and Eu/Eu^* values of samples from the Zunyi manganese deposits are 5.53–56.92, 18–39, 1.42–3.15, 0.55–2.20, 0.21–1.76 and 0.48–0.86, respectively, indicating a hydrothermal origin for the manganese mineralization and REEs enrichment. The $\delta^{13}C_{V\text{-}PDB}$ (−0.54 to −18.1‰) and $\delta^{18}O_{SMOW}$ (21.6 to 26.0‰) characteristics of manganese ores reveal a mixed source of magmatic and organic matter. Moreover, the manganese ore, tuffaceous clay rock and Emeishan basalt have extremely similar REE fractionation characteristic, suggesting REEs enrichment and manganese mineralization have been mainly origin from hydrothermal fluids.

Key words: Genesis, REEs enrichment, Hydrothemal origin, Permian manganese deposits, Zunyi

Citation: Xu et al., 2020. Genesis for Rare Earth Elements Enrichment in the Permian Manganese Deposits in Zunyi, Guizhou Province, SW China. Acta Geologica Sinica (English Edition), 94(1): 90–102. DOI: 10.1111/1755-6724.14338

1 Introduction

The area of southwestern China is one of the most important production areas for China's rare earth resources, in which the major industrial sources of rare earth deposit types include weathered basalt, granite, phosphorite, etc rock bodies with high REEs background values (Yang et al., 2008; Xie and Zhu, 2012; Huang et al., 2014; Zhang et al., 2016; Xu et al., 2017). In recent years, the soaring of global demand for rare earth resources, comprehensive research and utilization of associated rare earth resources has attracted much attention. Specially that most studies have noticed the anomalous enrichment of rare earth elements (REEs) in manganese deposits and has become a new focus in the field of geology (Kato et al., 2005a, b; Mohapatra et al., 2006; Mishra et al., 2006; Moriyama et al., 2008; Mongelli et al., 2013). Recently, through the analysis of REE compositions from the Zunyi manganese deposits, one unanticipated finding was the manganese ores universal possess high ΣREE contents with ranging from 158 to 1138.9 ppm (average 509.54 ppm) (Xu et al., 2018). The concentrations of ΣREE from Changzheng, Nancha and Tongziwo manganese deposits in Zunyi region range from 393.6 to 721 ppm, 158 to 823 ppm and 326.3 to 1138.9 ppm, respectively. In addition, comprehensive previous studies also found that the Permian manganese deposits from Zunyi to Qianxi and Nayong to Xuanwei region present generally enriched in

* Corresponding author. E-mail: gaojunbo1985@126.com

© 2020 Geological Society of China

REEs (Fig. 1; Liu et al., 2008; Yang et al., 2009; Liu et al., 2015), which display this area have great potential for rare earth mineralization.

The Permian manganese deposits from Zunyi area were initially discovered in 1944 near Zunyi city, which were the first manganese deposits with industrial value found in Guizhou Province (Liu et al., 1989; Liu et al., 2008). After more than half a century of systematic research had achieved significant progress in the origin, metallogenic regularities and prospecting exploration of manganese deposits (Liu et al., 1989; Fan and Yang, 1999; Liu et al., 2008; Liu et al., 2015; Gao et al., 2018). In recent years, two new large-scale and two medium-scale manganese deposits have been found in Zunyi area, indicating that Zunyi manganese ores belt has great potential for mineralization. However, previous studies focused only on the origin, metallogenic regularities and prospecting exploration of manganese deposits (Liu et al., 1989; Fan and Yang, 1999; Liu et al., 2008; Yang et al., 2009, 2018; Liu et al., 2015; Gao et al., 2018). In regarding to the enrichment characteristics, sources and enrichment mechanism of REEs in manganese deposits remain poorly understood. These aspects urgently require further research to complement work on the Zunyi manganese deposits and it associated REEs resources.

Therefore, we carried out integrated characterization of the ores deposits geology, petrology, mineralogy, electron probe microanalysis (EPMA), carbon and oxygen isotopic and element geochemistry of the Changzheng, Nancha, and Tongziwo manganese deposits. The results of this analysis have implications for the enrichment characteristics, metallogenic environment and material

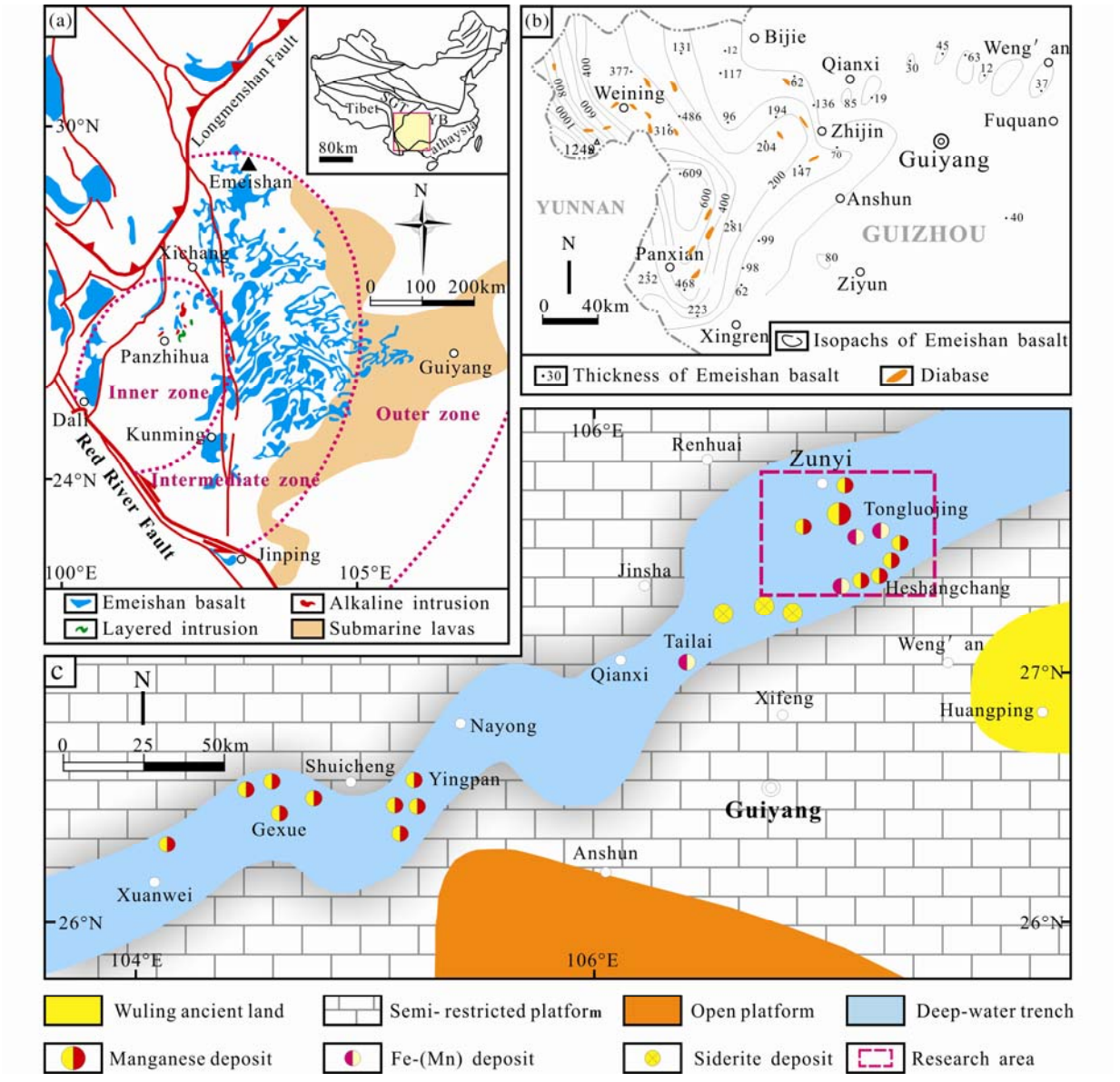


Fig. 1. Map showing distribution of Emeishan Large Igneous Province (ELIP) in southwest China and the map of lithofacies and paleogeography of Middle Permian manganese deposits in central-western Guizhou, SW China

(a) Distribution of ELIP in southwest China (after Ukstins-Peate et al., 2008); (b) distribution of ELIP in Guizhou (after Guizhou Bureau of Geology and Mineral Resources 1987); (c) distribution of lithofacies and Paleogeography and manganese deposits in central-western Guizhou (after Chen et al., 2003)

sources of the REEs in Zunyi manganese deposits and so facilitate a deeper understanding of the genesis of REEs enrichment.

2 Geological Settings

2.1 Regional geology

The Emeishan mantle plume activity peaked during the middle to late Permian and influenced magmatic activity across large portions of southwestern China (Ali et al., 2005; Zhou et al., 2006). Previous studies have documented that the main eruption timing of the Emeishan basalt was concentrated at ~260 Ma (Zhou et al., 2002, 2006; Guo et al., 2004; Ali et al., 2005; Zhong et al., 2006; Yumul et al., 2008; Tao et al., 2009; Zhong et al., 2014) and constrained the end of Emeishan volcanism to 251±0.1 Ma (Lo et al., 2002; Fan et al., 2004; Zhu et al., 2011). The intense activity of the Emeishan mantle plume had a profound influence on the paleogeography and paleotectonic evolution of Sichuan, Yunnan, Guizhou and surrounding areas (Fig. 1a; Ali et al., 2005; Hou et al., 2006; Song et al., 2009; Xu et al., 2014; Shellnutt, 2014; Huang et al., 2014; Li et al., 2015, 2017). Influenced by the regional deep fault and the paleogeographic situation, the Emeishan basalt expanded from west to east and affected the whole northwestern and central sections of Guizhou (Fig. 1b). The uplift of the Emeishan mantle plume produced significantly affected the crustal structure in the area, which formed a NE-NNE deep-water aulacogen crossing the Liupanshui fault depression and the Zunyi fault arch. Chen et al (2003) named it "aulacogen of central Guizhou" (Fig. 1c). The aulacogen of central Guizhou developed fold and fault systems with complex structural styles, and mainly developed the NE and NNE-trending syn-sedimentary faults (Fig. 2). The Permian manganese deposits in Zunyi-Shuicheng-Nanyong-Gexue area are strictly restricted within the aulacogen of central Guizhou, and the output shape and spacial distribution of the ore bodies are obviously controlled by the aulacogen (Liu et al., 1989; Hou, 1997; Yang et al., 2009; Liu et al., 2015, Gao et al., 2018).

2.2 Ore deposit geology

The Permian manganese deposits in Zunyi area located in the manganese-enriched zone on the southwestern margin of the Yangtze platform (Liu et al., 1989; Liu et al., 2008; Yang et al., 2009). The main outcrop strata in Zunyi manganese ores field is Cambrian, Ordovician, Silurian, Permian, Triassic, etc. In which, the lithology of the Upper Cambrian outcrop strata is the dolomite of Loushanguan formation. The Ordovician is dominated by dolomite, bioclastic limestone and siltstone. The Silurian is mainly consist of siltstone and shale. The overlying lithology is the Permian, is mainly made up of siliceous rocks, carbonaceous mudstone and limestone, and the Triassic consists of mudstone, marlite and dolomite (Gao et al., 2018). Influenced by the Duyun Movement (a tectonic movement between the late part of the end of the Ordovician and the early part of the early Silurian that resulted in missing strata, unconformities and disconformities), the "Central Guizhou Palaeouplift" went through a transformation stage from underwater to land uprisings during the late Ordovician (Deng et al., 2010; Gao et al., 2018), becoming part of the land and resulting in a lack of Devonian and Carboniferous strata in this area. The Permian Maokou Formation is the REEs and manganese ore-bearing strata. The Zunyi manganese deposits are mainly distributed in the core and the two limbs of the Tongluojing anticline or in the composite parts of the Tongluojing and Xiazi anticlinorium (Fig. 2; Liu et al., 1989; Liu et al., 2015). The ore bodies are stratiform or stratoid in shape, and hosted in the siliceous

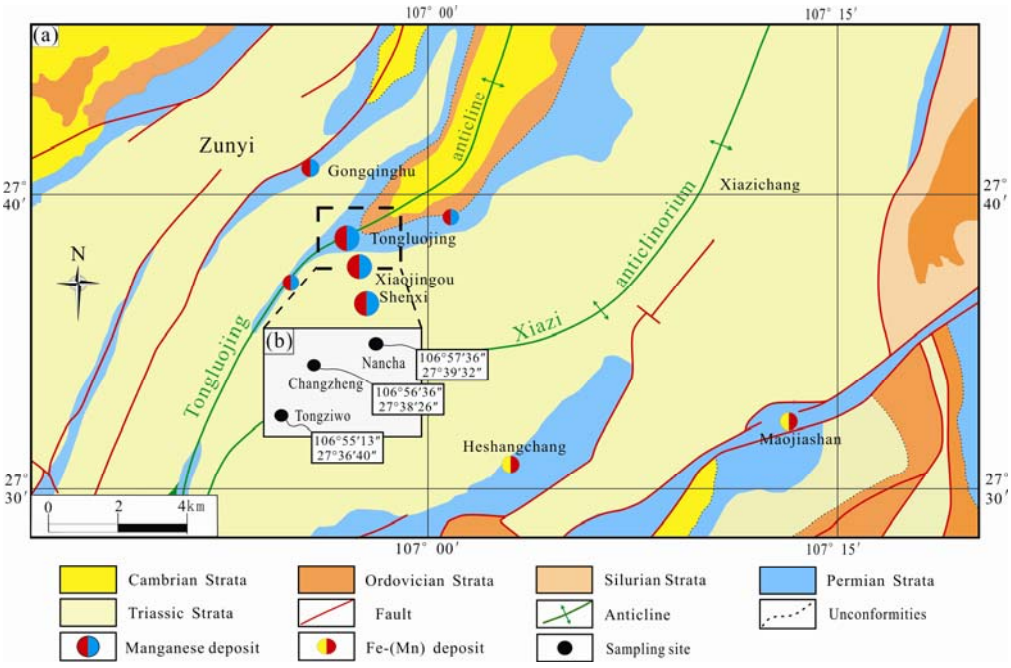


Fig. 2. Regional geological map of the Permian manganese deposits in the Zunyi region, Guizhou, SW China (Modified from Liu et al., 2015).

mudstones and carbonaceous rocks at the top of the Maokou Formation. The bottom of the manganese ore-bed is the "Bainitang layer", a siliceous rock Formation, which has a distribution area of approximately 900 km^2 and unequal thickness between 40 and 60 m surround distributed around manganese ore bodies in rings (Liu et al., 2008; Xu et al., 2017; Gao et al., 2018). The top of the manganese ore-bed is medium-thick layered bioclastic siliceous limestone. In addition, there are numerous of pyrite, illite, clay or carbonaceous clay rock developed in the transition zone between ore bed and bed top (Liu et al., 2008).

Research on the sedimentation structures and tectonic characteristics of the Zunyi manganese deposits reveal the coexistence of a variety of structures such as lamellar structure or massive structure (Fig. 3a), banded structure (Fig. 3b), brecciated structure (Fig. 3c–d) with an ascending order (Liu et al., 2008; Gao et al., 2018). In some cases, the brecciated structure also observed on basal of manganese deposit in Gexue area (Liu et al., 2008), but

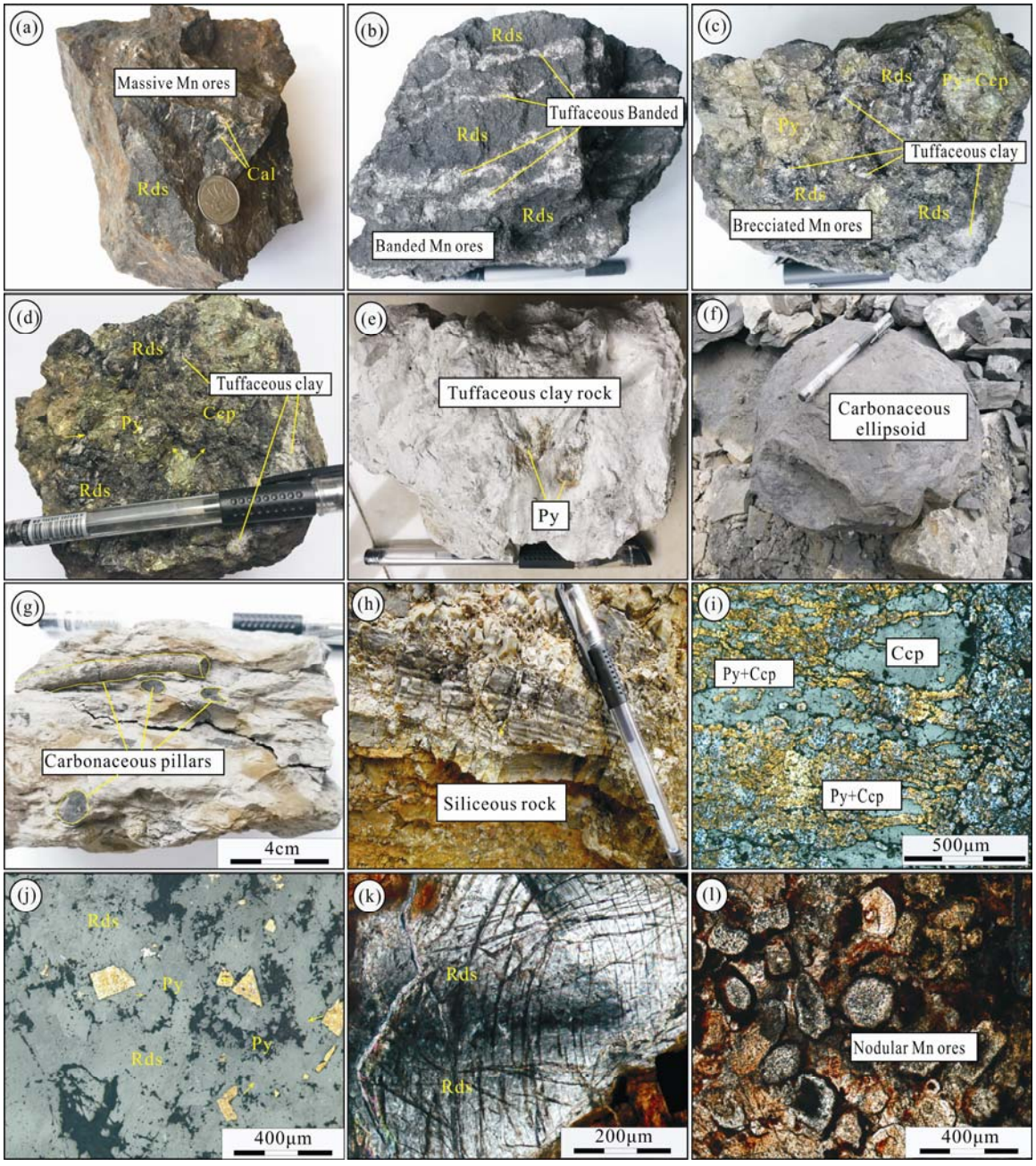


Fig. 3. Photographs showing typical feature of Permian manganese deposits at Zunyi, Guizhou Province.
(a) Steel gray massive manganese ore; (b) gray-black striped manganese ore; (c) gray-black brecciated manganese ore; (d) manganese ores closely coexisting with tuffaceous clay rock and brecciated pyrite; (e) tuffaceous clay rock; (f) black carbonaceous ellipsoid; (g) black carbonaceous pillars distributed in tuffaceous clay rock; (h) siliceous rock; (i) the veins, net vein pyrite - chalcopyrite mixed arrangement (cross-polarized light); (j) irregular granular pyrite (cross-polarized light); (k) the cleavage of rhodochrosite is obviously bent and deformed (cross-polarized light); (l) spherulitic rhodochrosite (cross-polarized light)

minor in Shuicheng-Nayong manganese deposits (Liu et al., 2013, 2015; Gao et al., 2018). The manganese ores closely coexisting with tuffaceous clay rock (Fig. 3b–d) and brecciated pyrite (Fig. 3b–e). Moreover, a black carbonaceous ellipsoid structure (approximately 5–30 cm in diameter) (Fig. 3f) and a carbonaceous pillar structure (approximately 1–10 cm in diameter) (Fig. 3g) were observed in the host rocks or tuffaceous clay rock.

The examines mineralogical and petrologic characteristics of manganese ore samples collected from Changzheng, Nancha and Tongziwo deposits in Zunyi region. The macro lithologies of most ore samples were apparent differentiated from the wall rocks due to their structures and appearance at the macro-scale (Fig. 3 a–h). The mainly the ore minerals consist of rhodochrosite, followed, in order of decreasing abundance, by calcimangite, capillitite and manganocalcite. Additionally, the ore bodies and wall rocks contain numerous of sulfides or sulfide assemblages, mainly pyrite (Fig. 3b–d), chalcopyrite (Fig. 3b–d), as well as barite, rutile, siliceous rock (Fig. 3h), tuffaceous clay rock and calcite also have been found in manganese ore (Liu et al., 2008; Gao et al., 2018). The microstructure features under the microscope display the coexistence of a variety of textures like veinlet texture (Fig. 3i, k), granule texture (Fig. 3j), pisolitic texture (Fig. 3l). In some case, capillitite present reddish-brown (Fig. 3l) and chalcopyrite present steady covellite (Fig. 3i) probably as a result of its iron content and oxidized. In addition, minerals of hydrothermal origin (e.g., rutile, barite, galena, sphalerite, pyrite and chalcopyrite) are also present in Zunyi manganese deposits (Liu et al., 2008; Gao et al., 2018). The occurrence of the mineral assemblage of barite, rutile, galena, sphalerite, brecciated pyrite, carbonaceous ellipsoid and carbonaceous pillar in Zunyi manganese deposits is comparable to those of characteristically hydrothermal deposit. These geological features are clearly distinct from normal marine manganese deposits but similar to typical hydrothermal manganese deposits (Liu et al., 2008; Liu et al., 2013, 2015; Papavassiliou et al., 2017; Gao et al., 2018).

3 Samples and Methods

Twenty-three samples of manganese ores and wall rocks (6 samples collected from the Changzheng manganese deposit (106° 56′ 36″ E, 27° 38′ 26″ N), 11 samples collected from the Nancha manganese deposit (106°55′13″E, 27°36′40″N), and 6 samples collected from the Tongziwo manganese deposit) (106°57′36″E, 27°39′ 32″N) were sampled from three manganese deposits in Zunyi, Guizhou Province. All of the samples include manganese ore, manganiferous limestone, siliceous rock and tuffaceous clay rock.

The rare earth elements (REEs) of 23 samples were analyzed by using a PE Elan6000 inductively coupled plasma mass spectrometer (ICP-MS) at an accredited laboratory (ALS Minerals-ALS Chemex Co. Ltd., Guangzhou, China). The experimental method involved dissolving samples with $HF+HNO_3$ after adding a Rh internal standard solution, converting them to a 1% HNO_3 solution, and measuring them with the ICP-MS. The analytical accuracy was better than 5%.

The EPMA and energy spectrum analysis of 3 manganese ore samples were performed by JXA-8100 at the Xi'an Center of Geological Survey, Geology Survey of China. The samples were ground into thin blocks and were spray coated with conductive carbonaceous thin films. The samples were analyzed with a JXA-8100 Inca Energy electron probe produced by Japan Electron Optics Laboratory. The experimental conditions are as follows: an acceleration voltage of 15 kV, a beam of 1.00×10^{-8} A, and a beam spot diameter of 1 μm. The scanning backscatter electron imaging technology of the electron probe under different magnifications was utilized to observe the phase composition of the sample surface and identify the microcomponents of the phase.

Carbon and Oxygen isotope analyses of 17 samples were carried out in the Key National Laboratory of Environmental Geochemistry of the Institute of Geochemistry under the Chinese Academy of Sciences. The instrument used was a gas-stable isotope mass spectrometer under continuous flow mode. The details as follows: (1) measure 1 mg ± 50 ug dried carbonate powder (based on $CaCO_3$), put it into a reaction bulb, tighten the shock insulator, and put the bulb in a sample tray at a temperature of 90.0 ± 0.1°C; (2) use a 30 ml/min helium flow for 5 min to eliminate air from the reaction bulb; (3) inject 300 μl of 100%-pure phosphoric acid into the branch duct of the reactor the phosphoric acid and carbonate react immediately, releasing CO_2 into the reaction bulb; (4) after the reaction is complete, use helium flow to purge the gas from the reaction bulb through a chromatographic separation column; and (5) guide the CO_2 into the IRMS and report as $\delta^{13}C$ and $\delta^{18}O$ values in ‰ notation relative to the VPDB (Vienna Pee Dee Belemnite) (carbon and oxygen) standard. During the analysis, carbonate solid standards are inserted for the purpose of calibrating the measurement results.

4 Results

4.1 REE compositions

The REEs compositions of the Changzheng, Nancha and Tongziwo manganese ores from Zunyi area are listed in Table 1. The ΣREE contents of the manganese ores range from 158 ppm to 1138.9 ppm, with an average of 509.54 ppm. Specifically, the ΣREE contents of the Changzheng manganese ores range from 393.6 to 721 ppm, with an average of 506.79 ppm; the ΣREE contents of the Nancha manganese ores range from 158 to 823 ppm, with an average of 437.86 ppm; and the ΣREE contents of the Tongziwo manganese ores have a relatively higher range of 326.3 ppm to 1138.9 ppm, with an average of 601.90 ppm. In particular, the ΣREE contents of the tuffaceous clay rock in manganese ores are the highest, which range from 1032.15 ppm to 1824.5 ppm, with an average of 1396.4 ppm. In comparison, the wall rocks show lower REE content, ranging from 22 to 297.9 ppm, with an average of 136.4 ppm. Therefore, the degrees of REE enrichment in the different types of manganese ores, wall rocks and tuffaceous clay rock have obvious

Table 1 REE compositions (ppm) of Permian manganese deposits from Zunyi region, Guizhou Province

Locality	Sample	Rock (ore) type	La	Ce	Pr	Nd	Sm	Eu	Gd	Tb	Dy	Ho	Er	Tm	Yb	Lu
Changzheng manganese deposit	cz01	Siliceous rock	13.80	33.40	4.34	19.10	3.88	0.92	3.34	0.46	2.35	0.45	1.29	0.19	1.03	0.17
	cz02	Manganese ore	222.00	108.00	43.20	186.00	32.40	6.37	35.50	5.30	32.40	7.45	20.70	2.93	16.30	2.48
	cz03	Manganese ore	103.00	121.00	22.00	85.00	16.45	2.86	11.10	1.57	8.94	1.86	5.81	1.14	10.80	2.04
	cz04	Manganese ore	90.40	254.00	15.15	57.90	12.35	2.24	9.20	1.40	7.44	1.34	3.45	0.48	3.41	0.41
	cz05	Manganese ore	76.80	260.00	15.90	62.00	13.10	2.08	7.93	1.15	6.01	1.16	3.08	0.46	3.23	0.49
	cz06	Siliceous shale	27.10	75.20	7.11	28.30	5.84	1.20	5.13	0.90	5.14	1.09	2.80	0.40	2.59	0.37
Nancha manganese deposit	nc01	Manganese ore	126.50	47.90	21.50	90.80	13.30	2.72	18.10	2.70	16.55	4.29	12.35	1.60	9.44	1.51
	nc01A	Manganese ore	112.00	42.80	19.35	82.70	12.80	2.92	19.20	2.80	18.25	4.45	12.85	1.64	9.31	1.52
	nc02A	Manganese ore	95.30	230.00	21.50	82.70	19.05	2.50	12.65	2.19	12.35	2.36	6.53	0.97	6.91	0.96
	nc02B	Manganese ore	142.50	434.00	32.50	131.00	28.50	4.01	18.35	2.58	12.85	2.36	6.51	0.95	6.44	0.91
	nc03	Siliceous shale	77.60	259.00	19.65	79.70	15.75	2.67	9.73	1.47	7.44	1.43	3.81	0.58	3.98	0.51
	nc04	Manganese ore	27.20	89.60	4.94	18.70	4.14	1.38	3.41	0.51	3.06	0.63	1.98	0.29	1.90	0.28
	nc06	Siliceous rock	89.10	85.70	15.25	63.20	11.60	2.11	10.75	1.39	7.89	1.57	4.15	0.59	3.80	0.56
	nc09	Tuff-clay rock	469.00	718.00	93.30	378.00	70.00	12.50	41.60	4.65	19.40	3.14	7.19	0.95	5.91	0.88
	nc10	Tuff-clay rock	255.00	401.00	50.60	209.00	47.80	8.72	28.50	3.06	13.65	2.35	5.60	0.84	5.29	0.74
	nc11	Tuff- clay rock	307.00	491.00	62.40	250.00	53.60	9.45	31.70	3.64	16.20	2.69	6.46	0.94	6.22	0.83
	nc12	Tuff-clay rock	378.00	579.00	76.80	307.00	61.20	10.50	36.10	4.12	17.25	2.86	6.54	0.90	5.80	0.83
Tongziwo manganese deposit	tzw01C	Siliceous rock	20.60	34.10	4.26	16.20	3.02	0.27	2.42	0.36	2.07	0.40	1.01	0.14	0.96	0.15
	tzw02B	Siliceous rock	8.80	8.60	1.32	5.50	0.98	0.24	0.98	0.13	0.99	0.22	0.57	0.06	0.40	0.07
	tzw03	Manganese ore	85.00	50.80	19.60	80.20	18.10	3.62	19.95	3.15	18.40	4.11	11.25	1.52	9.22	1.42
	tzw05A	Manganese ore	105.00	224.00	22.80	91.50	20.30	4.31	23.00	3.26	18.00	3.25	8.54	1.15	6.94	0.97
	tzw05B	Manganese ore	167.50	488.00	46.90	205.00	51.80	10.85	53.60	8.62	48.30	9.61	23.70	3.18	19.25	2.63
	tzw06	Manganese ore	91.80	110.50	20.90	83.70	19.75	4.15	20.60	3.67	21.50	4.56	12.55	1.93	11.90	1.79

Locality	Sample	Rock (ore) type	Y	ΣREE+Y	LREE	HREE	LREE/HREE	$(La/Yb)_{ch}$	Y/Ho	Ce_{anom}	Ce/Ce*	Eu/Eu*	$(La/Nd)_N$	$(Dy/Yb)_N$
Changzheng manganese deposit	cz01	Siliceous rock	11.70	96.42	75.44	9.28	8.13	9.61	26.00	−0.01	1.05	0.76	1.42	1.53
	cz02	Manganese ore	258.00	979.03	597.97	123.06	4.86	9.77	35.00	−0.62	0.25	0.57	2.35	1.33
	cz03	Manganese ore	42.70	436.27	350.31	43.26	8.10	6.84	23.00	−0.24	0.59	0.61	2.39	0.55
	cz04	Manganese ore	35.00	494.17	432.04	27.13	15.92	19.02	26.00	0.17	1.53	0.62	3.08	1.46
	cz05	Manganese ore	29.90	483.29	429.88	23.51	18.28	17.06	26.00	0.22	1.73	0.58	2.44	1.25
	cz06	Siliceous shale	29.10	192.27	144.75	18.42	7.86	7.51	27.00	0.10	1.30	0.66	1.89	1.33
Nancha manganese deposit	nc01	Manganese ore	160.50	529.76	302.72	66.54	4.55	9.61	37.00	−0.71	0.21	0.54	2.75	1.17
	nc01A	Manganese ore	175.00	517.59	272.57	70.02	3.89	8.63	39.00	−0.71	0.21	0.57	2.67	1.31
	nc02A	Manganese ore	43.30	539.27	451.05	44.92	10.04	9.89	18.00	0.07	1.20	0.46	2.27	1.20
	nc02B	Manganese ore	52.40	875.86	772.51	50.95	15.16	15.87	22.00	0.16	1.50	0.50	2.14	1.34
	nc03	Siliceous shale	27.90	511.22	454.37	28.95	15.69	13.99	20.00	0.18	1.58	0.61	1.92	1.25
	nc04	Manganese ore	15.70	173.72	145.96	12.06	12.10	10.27	25.00	0.23	1.76	1.09	2.87	1.08
	nc06	Siliceous rock	47.50	345.16	266.96	30.70	8.70	16.82	30.00	−0.31	0.52	0.57	2.78	1.39
	nc09	Tuff-clay rock	59.60	1884.12	1740.80	83.72	20.79	56.92	19.00	−0.12	0.79	0.65	2.44	2.20
	nc10	Tuff-clay rock	48.00	1080.15	972.12	60.03	16.20	34.58	20.00	−0.11	0.81	0.67	2.40	1.73
	nc11	Tuff- clay rock	54.00	1296.13	1173.45	68.68	17.00	35.40	20.00	−0.10	0.82	0.65	2.42	1.74
	nc12	Tuff-clay rock	58.80	1545.70	1412.50	74.40	18.90	46.75	21.00	−0.12	0.79	0.63	2.43	1.99
Tongziwo manganese deposit	tzw01C	Siliceous rock	10.20	96.16	78.45	7.51	10.45	15.39	26.00	−0.08	0.85	0.30	2.51	1.44
	tzw02B	Siliceous rock	8.30	37.16	25.44	3.42	7.44	15.78	38.00	−0.28	0.55	0.74	3.15	1.66
	tzw03	Manganese ore	105.50	431.84	257.32	69.02	3.73	6.61	26.00	−0.55	0.29	0.58	2.09	1.34
	tzw05A	Manganese ore	91.30	624.32	467.91	65.11	7.19	10.85	28.00	0.01	1.07	0.61	2.26	1.74
	tzw05B	Manganese ore	254.00	1392.94	970.05	168.89	5.74	6.24	26.00	0.09	1.33	0.62	1.61	1.68
	tzw06	Manganese ore	98.80	508.10	330.80	78.50	4.21	5.53	22.00	−0.24	0.59	0.62	2.16	1.21

Notes: Part of data are derived from Xu et al (2018). $Ce/Ce^{*}=2\times Ce_N/(La_N+Pr_N)$, $Ce_{anom}=lg[3Ce_{shale}/(2\times La_{shale}+Nd_{shale})]$, where N indicates that ratios were normalized to chondrite (Sun and McDonough 1989), PAAS indicates that ratios were normalized to post-Archean average Australian shale (Taylor and Mclennan 1985).

differences. The highest REE contents obtained in this study (up to 1824.50 ppm) are in tuffaceous clay rock from the Nancha deposit, followed by the brecciated and banded manganese ores (Xu et al., 2018).

4.2 Electron probe analyses

Representative EPMA data from the rhodochrosite from Zunyi manganese deposits are listed in Table 2. The REEs in Zunyi manganese deposits mainly occur in independent minerals (e.g., monazite, xenotime, etc.), which are euhedral-subhedral (Fig. 4a and b), veinlets (Fig. 4c) or porphyritic (Fig. 4d) distributed in the interior or cut through the pyrite and rhodochrosite. These features indicate directly that the REEs were deposited in a hydrothermal fluid, which was probably derived from regional hidden hydrothermal sources. The REEs composition in manganese ores is characterized by La, Ce and Nd enrichment in the Zunyi manganese deposits (Fig. 4e), and the heavy REE (HREE) Y are relatively enriched in a portion of the ore beds. Therefore, the REE compositions in Zunyi manganese deposits are mainly characterized by light REE (LREE) enrichment.

4.3 Carbon and oxygen isotopes analyses

The carbon and oxygen isotopic compositions of manganese deposit from Changzheng, Nancha and

Table 2 Representative EPMA data (wt%) of the rhodochrosite from Zunyi manganese deposits, Guizhou Province

Sample	Mineral	Point position	P_2O_5	SiO_2	Y_2O_3	La_2O_3	Ce_2O_3	Sm_2O_3	Pr_2O_3	Nd_2O_3	Gd_2O_3	Eu_2O_3	ThO_2	UO_2	Total
nc02-2	Rhodochrosite	Core	28.29	0.05	0.28	17.96	35.11	1.14	2.17	8.91	1.1	0.07	0.02	0.08	95.17
nc02-3	Rhodochrosite	Core	26.96	0.08	0.17	18.8	34.88	1.27	2.51	8.82	0.57	0	0	0	94.05
nc02-4	Rhodochrosite	Core	29.11	0.22	0.27	19.29	31.52	1.57	2.8	8.91	0.56	0	0	0.05	94.3
tzw05-10	Rhodochrosite	Core	27.35	1.83	0.07	8.02	33.69	3.13	2.71	16.92	1.19	0	0.18	0	95.07

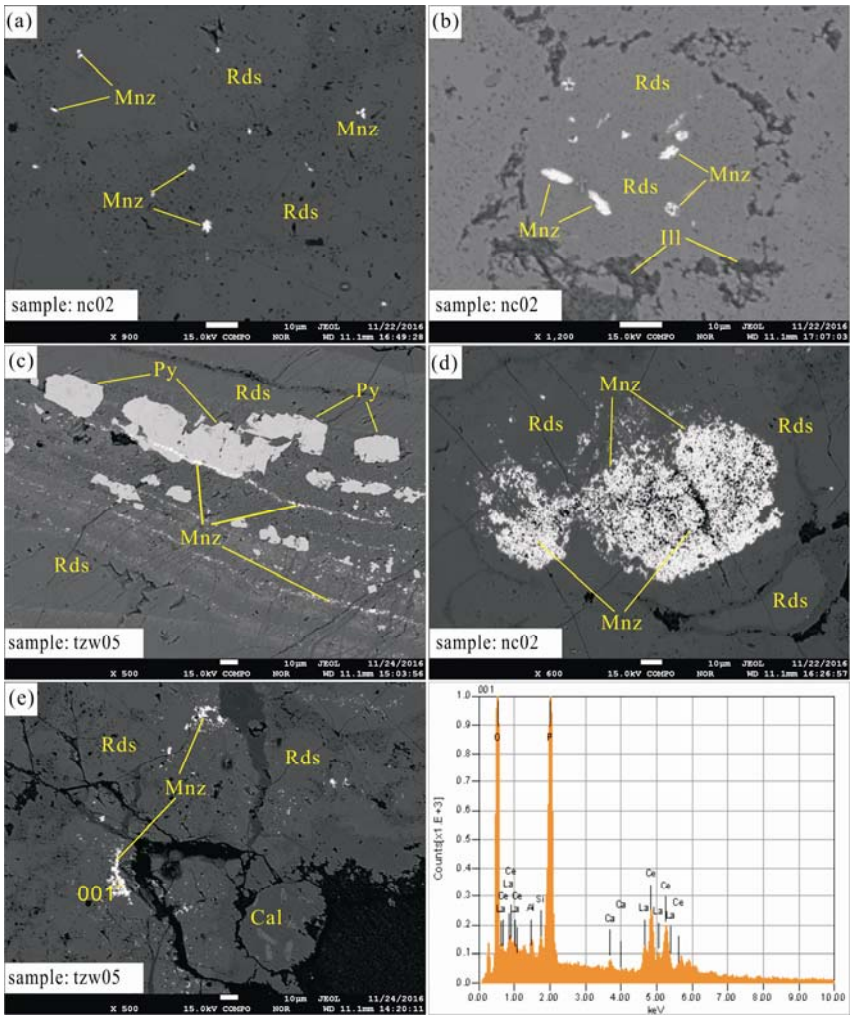


Fig. 4. The photos electron of Electron probe backscatter and X ray energy spectrum of Rhodochrosite.
(a) Monazite (Mnz) dispersively distributed in rhodochrosite (Rds); (b) monazite (Mnz) distributed in the rhodochrosite (Rds) as striped; (c) monazite (Mnz) is disseminated or veinlets cut through the pyrite (Py) and rhodochrosite (Rds); (d) Monazite (Mnz) distributed in rhodochrosite (Rds) as porphyritic; (e) the X-ray energy spectrum of monazite (Mnz) in rhodochrosite (Rds).

Tongzhiwo are listed in Table 3. The $\delta^{13}C_{V\text{-}PDB}$ values and $\delta^{18}O_{V\text{-}PDB}$ values of the manganese ores range from −18.152‰ to −0.547‰ (average −7.779‰) and −6.875‰ to −4.694‰ (average −5.794‰), respectively. In detail, the manganese ores from Nancha to Tongziwo to Changzheng exhibit $\delta^{13}C_{V\text{-}PDB}$ values of −18.152‰ to −0.547‰ (average −9.067‰), −13.571‰ to −4.241‰ (average −8.11‰) and −11.465‰ to −2.493‰ (average −5.837‰), as well as $\delta^{18}O_{V\text{-}PDB}$ values of −6.08‰ to −5.581‰ (average −5.785‰), −5.939‰ to −4.963‰ (average −5.496‰), and −6.875‰ to −4.694‰ (average −6.102‰), respectively. Besides, the $\delta^{13}C_{V\text{-}PDB}$ values and $\delta^{18}O_{V\text{-}PDB}$ values of the Siliceous rock varies from 1.091‰ to 3.902‰ (average 2.469‰) and −8.988‰ to −6.364‰ (average −7.149‰), respectively.

5 Discussions

5.1 Sedimentary environment of REEs

Wright and Holser (1987) proposed that Ce_{anom}. (Ce_{anom}= $lg[3Ce_{PAAS}/(2 \times La_{PAAS}+ Nd_{PAAS})]$ is a good index to reflects oxidation-reduction condition for the depositional environment. Generally, $Ce_{anom} > -0.1$ indicates that the water body within which the manganese ores formed or deposited was deficient in oxygen, whereas $Ce_{anom} < -0.1$ indicates that the sedimentary water body was oxidative (Wright and Holser, 1987). The Ce_{anom}. ratios of the manganese ores from Zunyi area all cover a

Table 3 The carbon and oxygen isotopic compositions of the Permian manganese deposits from the Zunyi region, Guizhou Province

Locality	Rock (ore) type	Sample	$\delta^{13}C$ ($_{V\text{-}PDB}$,‰)	$\delta^{18}O$ ($_{V\text{-}PDB}$,‰)	$\delta^{18}O$ ($_{SMOW}$,‰)
Nancha manganese ores	Manganese ore	nc01A	−15.938	−5.581	25.157
	Manganese ore	nc02A	−7.581	−5.787	24.944
	Manganese ore	nc02B	−3.12	−5.836	24.894
	Manganese ore	nc01	−18.152	−5.644	25.092
	Manganese ore	nc04	−0.547	−6.08	24.642
	Siliceous rock	nc05	2.201	−8.988	21.644
Tongziwo manganese ores	Siliceous rock	tzw01A	2.928	−7.142	23.547
	Siliceous rock	tzw01B	3.902	−6.464	24.246
	Siliceous rock	tzw01C	2.226	−6.791	23.909
	Manganese ore	tzw03	−8.303	−4.963	25.794
	Manganese ore	tzw06A	−4.241	−5.415	25.328
	Manganese ore	tzw05A	−6.325	−5.939	24.787
	Manganese ore	tzw05B	−13.571	−5.668	25.067
Changzheng manganese ores	Manganese ore	cz02	−5.868	−4.694	26.071
	Manganese ore	cz03	−11.465	−6.559	24.148
	Manganese ore	cz04	−3.524	−6.875	23.823
	Manganese ore	cz05	−2.493	−6.281	24.435
	Siliceous shale	cz06	1.091	−6.364	24.349

large range from −0.71 to 0.23 (average −0.13), but overall present negative Ce_{anom} indicates that manganese and REE were precipitate in a weak oxidition-reduction environment. Gao et al. (2018) suggests that the paleo sedimentary environment experienced long term, dramatic variations during ore-forming processes, and these fluctuations may be linked to periodic crust uplift and subsidence resulting from volcanism in Zunyi and its adjacent areas during the Middle to Late Permian.

Comprehensive the research of lithofacies and paleogeography, the Zunyi area located in the deep-water environment of aulacogen of central Guizhou during the Middle to Late Permian (Liu et al., 1989; Liu et al., 2015; Gao et al., 2018; Yang et al., 2018). The aulacogen of central Guizhou was controlled by region deep faults and had a water depth of more than 60 m, but on both sides was shallow-water restricted carbonate platform facies with water depths of less than 10 m (Chen et al., 2003; Gao et al., 2018) which reflect a weak oxidition-reduction transitional environment. This is consistent with geochemical characteristics, indicating the REEs and manganese deposition should be taken place in a weak oxidition-reduction environment. Additional, previous studies of Zunyi manganese ores and "Bainitang layer" siliceous rocks also support that the metallogenic environment for Zunyi manganese deposits was a weak oxidition-reduction environment (Xu et al., 2017; Gao et al., 2018). Due to the weak oxidation environment are beneficial for the deposition of some insoluble Mn^{4+} as oxides or hydroxides (Wu et al., 2016), while the large area of siliceous rocks at the bottom of Zunyi manganese deposits played a protective role in the preservation of the manganese and REE (Liu et al., 2013). Therefore, the deep -water aulacogen of central Guizhou provided an important reservoir space and favorable metallogenic conditions for manganese and REE enrichment and mineralization.

5.2 Sources of the rare earth elements (REEs)

Previous studies have documented that the extensive distribution area of Emeishan basalt is one of the areas that is relatively enriched in REEs, rare elements and dispersed elements in southwestern China (Yang et al., 2008; Zhou et al., 2013; Zhang et al., 2016). These manganese deposits within the aulacogen of central Guizhou, such as Zunyi, Shuicheng, Qianxi and Gexue (Yunnan), are formed in the middle-outer zone of the Emeishan Large Igneous Province (ELIP), and widely distribution of volcanic tuffaceous materials and more complex syn-sedimentary fault systems (Liu et al., 1989; Liu et al., 2008; Gao et al., 2018; Yang et al., 2018). In addition, these manganese deposits present many mineral assemblages associated with hydrothermal sedimentation in manganese ores deposits, such as, rutile, barite, galena, sphalerite, pyrite, and carbonaceous column etc (Liu et al., 2008; Gao et al., 2018). The map of Electron probe backscatter reveal monazite as disseminated or veinlets cut through the pyrite and rhodochrosite (Fig. 4 a–c), indicating directly that the REEs were deposited in a hydrothermal fluid, which was probably derived from regional hidden hydrothermal sources. It is noteworthy that, the ΣREE contents of these manganese deposits are significantly high, such as Zunyi (ΣREE=509.54 ppm, tuffaceous clay rock=1394 ppm), Shuicheng (ΣREE=712 ppm), Qianxi (ΣREE=1175.11 ppm) and Xuanwei (ΣREE=493 ppm) (Table 4; Liu et al., 2008; Yang et al., 2009; Xu et al., 2018). This is similar to the hydrothermal manganese deposits in Sardinia, Western Italy (REE= 3309.15 ppm) (Mongelli et al., 2013), the Neptuno manganese deposits in the Santa Rosalía basin and adjacent areas in Baja California Sur, México (REE=563.10 ppm) (Del RioSalas et al., 2008), and the late Archean hydrothermal HREE-rich manganese deposit in eastern India (REE highest=563.10 ppm) (Mohapatra et al., 2006; Mishra et al., 2006; Moriyama et al., 2008). Hence, these obvious geological and geochemically characteristics indicate that manganese mineralization and REEs enrichment have been related to hydrothermal activity in Zunyi and its adjacent areas during the middle to late Permian.

The studied ore samples have higher ΣREE concentrations (ΣREE=158–1824 ppm, average 509.54 ppm) and increased fractionation of light REEs (LREE) and heavy REEs (LREE/HREE=3.73–18.28, average 10.65), with higher $(La/Yb)_{ch}$ ratios of 5.53–56.92 (average16.91), reflect interaction with the highly evolved comenditic lava, this is consistent with the REE fractionation characteristics of the hydrothermal manganese ores (Michard, 1989; German et al., 1990; Maynard, 2010; Sinisi et al., 2012; Mongelli et al., 2013). Moreover, the Y/Ho values of the studied ore samples range from 18 to 39, with an average of 25.5, which are significantly lower than those of normal seawater (44–74) (Bau et al., 1999) but close to volcanic rocks (26–28) (Nozaki et al., 1997; Liakopoulos et al., 2001; Nyame et al., 2002; Oksuz, 2011; Wu et al., 2016). In hydrothermal fluids $(La/Nd)_N$ ratio is 3.0–7.4 (average 4.5) and $(Dy/Yb)_N$ ratio is 0.6–2.1 (average 1.2) (Fitzgerald and Gillis, 2006; Oksuz, 2011). The ranges of $(La/Nd)_N$ and $(Dy/Yb)_N$ ratio

for the Zunyi manganese deposits are 1.42–3.15 (average 2.37) and 0.55–2.20 (average 1.43), respectively, which are distinctly different from normal seawater, but are close to those of hydrothermal fluids. These fractionation characteristics indicate a hydrothermal origin for the manganese mineralization and REEs enrichment, as well as the mineralization processes of Zunyi manganese deposits were obviously influenced by hydrothermal activity related to volcanism.

On average, the hydrothermal manganese ores general have large Ce/Ce* fluctuations (Oksuz, 2011; Mongelli et al., 2013), because in addition to the fluid composition, the concentration of REEs in hydrothermal fluids is controlled by temperature, pressure, Eh, pH, crystallo-chemical factors, and reaction kinetics, etc (Haas et al., 1995; Gieré, 1996; Mongelli et al., 2013). The Ce/Ce* values of Zunyi manganese deposits ranges from 0.21 to 1.76(average 0.93) display a large Ce/Ce* fluctuations, and the Eu/Eu* values of Zunyi manganese deposits ranges from 0.30 to 1.09 (average 0.62). This is similar to manganese deposits associated with hydrothermal activity in Sardinia, Western Italy (Ce/Ce*=0.35–3.15, average 1.42; Eu/Eu*=0.01–0.67, average 0.26), and close to the hydrothermal deposits from Baby Bare seamount in the Northeast Pacific Ocean (Ce/Ce*=0.22–2.37, average 1.02; Eu/Eu*=0.48–0.86, average 0.68) (Fitzgerald and Gillis, 2006; Oksuz, 2011; Mongelli et al., 2013; Xie et al., 2013). Furthermore, In the (Ce/Ce*) vs. (Pr/Pr*) plot (Bau and Dulski, 1996), the measured compositions of the manganese ores from Zunyi area fall close to or on the modeled curve (Fig. 5). Previous studies suggested that involves the precipitation of newly formed REE-bearing minerals, including cerianite, within the Mn-ores from the hydrothermal fluids, resulting in positive Ce anomalies; and precipitation of REE-bearing minerals from the Ce-depleted hydrothermal fluid, giving rise to negative Ce anomalies (Ramos Preston, 2001; Vaniman et al., 2002; Chetty and Gutzmer's, 2012; Mongelli et al., 2013). This is consistent with the occurrence of apatite, monazite, and cerianite, which grew within Zunyi manganese ore (Fig. 4). Therefore, the Ce/Ce* and Eu/Eu* values suggest that hydrothermal activity played an important role in the processes of manganese mineralization and REEs enrichment.

Previous studies have documented that the Permian seawater have lower ΣREE concentrations (roughly 1.53 ppm), with negative Eu and Ce anomalies, and its REE model is characterized by relatively flat of REE distribution patterns (Kawabe et al., 1991; Gao et al., 2018). Ore samples of the Zunyi manganese deposits have high ΣREE concentrations (509.54 ppm), with large Ce anomalies fluctuations but overall display a weakly negative Ce anomalies and obvious negative Eu anomalies, and its REE model is characterized by a weakly right-oblique nature of REE distribution patterns (Fig. 6a) that distinctly different from the Permian

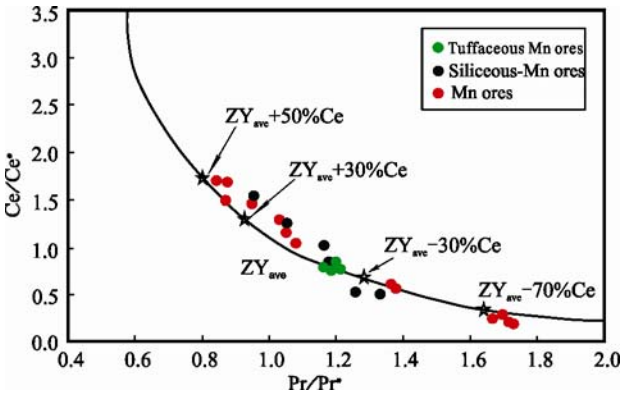


Fig. 5. Ce/Ce* vs. Pr/Pr* plot of Permian manganese ores in Zunyi area, Guizhou Province.

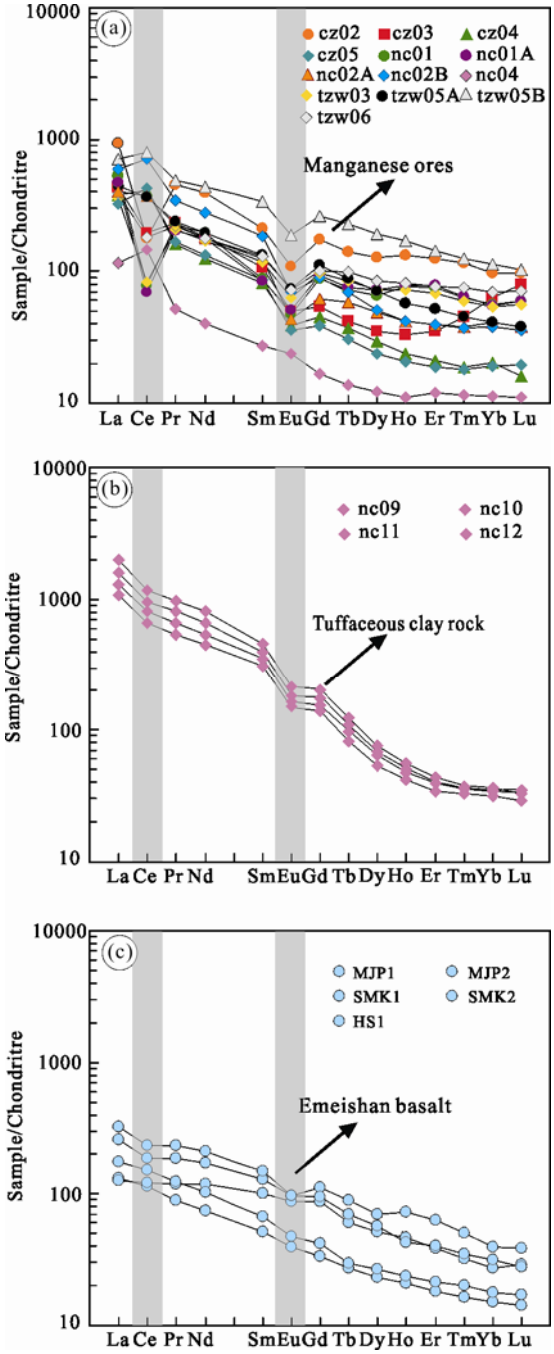


Fig. 6. Chondrite-normalized REE patterns of all samples. Chondrite data are from (Sun and McDonough, 1989).
(a) Changzheng, Nancha and Tongziwo manganese ores; (b) tuffaceous clay rock from Nancha manganese deposit; (c) wmeishan basalt from the Norhtwest Guizhou (after Zheng Lulin unpublished data)

seawater. It's also worth further discussion is the tuffaceous clay rock that closely coexisting with manganese ores (Fig. 2b–e) in Zunyi manganese deposits. Compared with manganese ores, the samples of tuffaceous clay rock have higher ΣREE concentrations (1396.42 ppm), with a weakly negative Ce and Eu anomalies, and its REE model is characterized by right-oblique nature of REE distribution patterns (Fig. 6b) that similar to the samples of manganese ores. In addition, both manganese ores and tuffaceous clay rocks are characterized by La, Ce, Nd and Y enriched (Table 1). This result imply they have the same of material source or source region, and the hydrothermal processes related to volcanic eruption maybe played an important role in REEs enrichment and manganese mineralization. Moreover, the samples of manganese ores and tuffaceous clay rocks also display similar of REE fractionation characteristics with the Emeishan basalt from northwestern Guizhou Province (Fig. 6c). In addition to the obvious lower of REE concentrations than manganese ores and tuffaceous clay rocks, the Emeishan basalt present a weakly negative Ce and Eu anomalies with a weakly right-oblique nature of REE distribution patterns, this is similar to the samples of manganese ores and tuffaceous clay rocks. Thus, these REE fractionation characteristics indicate REEs enrichment and manganese mineralization in Zunyi manganese deposits appear to have been mainly sourced from hydrothermal activity.

Most studies have clarified the marine sedimentary carbonates $\delta^{13}C_{V\text{-}PDB}$ values −1‰ to +2‰ (average, 0‰) and magmatic rocks or volatile $\delta^{13}C_{V\text{-}PDB}$ values −2‰ to −11‰ (Hein and Kosk, 1987; Taylor, 1986; Hoefs, 1997; Zeng and Liu, 1999; Zheng and Chen, 2000; Chen et al., 2017), as well as organic matter $\delta^{13}C_{V\text{-}PDB}$ values −10‰ to −19‰ (Hoefs, 1997; Chen and Wang, 2004). The $\delta^{13}C_{V\text{-}PDB}$ values of ore samples in Zunyi manganese deposits range from −0.54‰ to −18.1‰ (Table 3). The $\delta^{13}C_{V\text{-}PDB}$ values of manganese ores samples obvious lower than the sample of siliceous rock in Zunyi region, and are mainly plot in the field of mantle, yet minority plot in the field of organic matter (Fig. 7). The carbon isotopic compositions present a large difference in manganese ores is probably the result of the mixing of deep carbon source and organic carbon source. This result indicate that the sources of hydrothermal fluids and organic matter have been involved in the REEs enrichment and manganese metallogenesis (Hoefs, 1997; Okita et al., 1988; Yeh, 1999; Lafaye and Weber, 2003; Xie et al., 2013; Chen et al., 2017). The $\delta^{18}O_{smow}$ average values of all samples is 25.63‰ with maximum and minimum values of 26.07‰ and 21.64‰ respectively, which is partly beyond the area for marine organic matter (Fig. 7) and exhibit a tendency to magmatic rocks (Pfeifer et al., 1988; Xie et al., 2013; Chen et al., 2017). The carbon and oxygen isotopic data indicate that a mixed source of hydrothermal fluids and organic matter have been involved in the manganese mineralization and REEs enrichment in Zunyi manganese deposits.

6 Conclusions

(1) The Zunyi manganese deposits are generally enriched in LREE, and the concentrations of ΣREE in manganese ores range from 158 to 1138.9 ppm, with an average of 509.5 4 ppm. The REEs in the manganese ores are characterized by La, Ce and Nd enriched, and exist in the form of monazite and xenotime ect.

(2) The Ce_{anom} ratios (average −0.13) and lithofacies and paleogeography characteristics indicate that Zunyi manganese deposits were formed in a weak oxidition-reduction environment.

(3) The manganese ores have high concentrations of REEs (158–1824 ppm), and the LREE/HREE (3.73–18.28), $(La/Yb)_{ch}$ ratios (5.53–56.92), Y/Ho(18–39) ratios, $(La/Nd)_N$ ratio (1.42–3.15) and $(Dy/Yb)_N$ ratio (0.55–2.20), Ce/Ce^* values (0.21–1.76), Eu/Eu^* values (0.48–0.86) support the involvement of hydrothermal input during enrichment of the REEs and manganese.

(4) The $\delta^{13}C_{V\text{-}PDB}$ (−0.54 to −18.1‰) and $\delta^{18}O_{SMOW}$ (21.6–26.0‰) index of Zunyi manganese deposits reveal a mixed source of hydrothermal fluids and organic matter. The REE fractionation characteristics of Zunyi manganese ores are similar to tuffaceous clay rock and Emeishan basalt, indicating that manganese mineralization and REEs enrichment have been mainly sourced from hydrothermal activity.

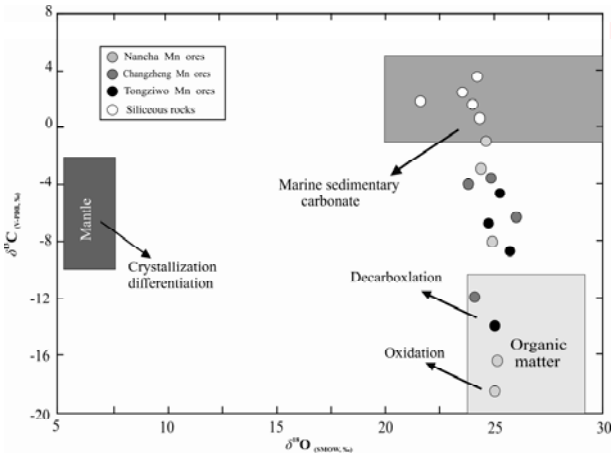


Fig. 7. C-O isotopic components diagram of Permian manganese deposits in the Zunyi region, Guizhou.
Siliceous rocks samples of Permian manganese deposits plot in the field of marine sedimentary carbonate, almost all of manganese ore samples fall in the field of magmatic rocks (or volatile) and organic matter, indicating two manganese-forming sources. Data source: Mantle (Harmon and Hoefs 1995; Taylor 1986; Zheng and Chen, 2000); Marine sedimentary carbonate (Hoefs 1997); organic matter (Hoefs, 1997; Chen and Wang, 2004)

Acknowledgments

This research was financially supported by the project of the graduate scientific research fund of Guizhou Province (No. KYJJ2017009), the National Natural Science Foundation of China (No. U1812402), the project of the scientific and technological innovation team of sedimentary deposits in Guizhou Province (No. 2018-5613) and the Project of Talent Base in Guizhou Province (No. RCJD2018-21).

Manuscript received Nov. 27, 2018
Accepted Mar. 5, 2019
associate EIC FEI Hongcai
edited by FEI Hongcai

References

Ali, J.R., Thompson, G.M., Zhou, M.F., and Song, X.Y., 2005. Emeishan Large Igneous Province, SW China. Lithos, 79(3): 475–489.

Bau, M., and Dulski, P., 1996. Distribution of yttrium and rare-earth elements in the Penge and Kuruman iron-formations, Transvaal Supergroup, South Africa. Precambrian Research, 79(1–2): 37–55.

Bau, M., and Dulski, P., 1999. Comparing yttrium and rare earths in hydrothermal fluids from the Mid-Atlantic Ridge: implications for Y and REE behaviour during near-vent mixing and for the Y/Ho ratio of Proterozoic seawater. Chemical Geology, 155(1–2): 77–90.

Chen, F.G., Wang, Q.F., Yang, S.J., Zhang, Q.Q., Liu, X.F., Chen, J.H., and Carranza, E., 2017. Space-time distribution of manganese ore deposits along the southern margin of the South China Block, in the context of Palaeo-Tethyan evolution. International Geology Review, 60: 1–15.

Chen, J., and Wang, H.N., 2004. Geochemistry. Beijing: Science Press, 129 (in Chinese).

Chen, W.Y., Liu, J.R., Wang, Z.G., and Zheng, Q.L., 2003. Study on lithofacies palaeogeography during the Permian Emeishan basalt explosion in Guizhou Province. Journal of Palaeogeography, 5(1): 17–28. (in Chinese with English abstract)

Chetty, D., and Gutzmer, J., 2012. REE redistribution during hydrothermal alteration of ores of the Kalahari manganese deposit. Ore Geology Reviews, 47(5): 126–135.

Del RioSalas, R., Ruiz, J., Ochoa-Landín, L., Noriega, O., Barra, F., Meza-Figueroa, D., and Paz-Moreno, F., 2008. Geology, Geochemistry and Re–Os systematics of manganese deposits from the Santa Rosalía Basin and adjacent areas in Baja California Sur, México. Mineralium Deposita, 43(4): 467–482.

Deng, X., Yang, K.G., Liu, Y.L., and Sheng, Z.B., 2010. Characteristics and tectonic evolution of Qianzhong Uplift. Frontiers of Earth Science, 17(3): 79–89 (in Chinese with English abstract).

Fan, D.L., and Yang, P.J., 1999. Introduction to and classification of manganese deposits of China. Ore Geology Reviews, 15(1–3): 1–13.

Fan, W.M., Wang, Y.J., Peng, T.P., Miao, L.C., and Guo, F., 2004. Ar-Ar and U-Pb geochronology of late Paleozoic basalts in western Guangxi and its constraints on the eruption age of Emeishan basalt magmatism. Chinese Science Bulletin, 49 (18): 2318–2327 (in Chinese with English abstract).

Fitzgerald, C.E., and Gillis, K.M., 2006. Hydrothermal manganese oxide deposits from Baby Bare seamount in the Northeast Pacific Ocean. Marine Geology, 225(1–4): 145–156.

Gao, J.B., Yang, R.D., Xu, H., Zhang, X., Chen, J., and Zheng, L.L., 2018. Genesis of Permian sedimentary manganese deposits in Zunyi, Guizhou Province, SW China: Constraints from geology and elemental geochemistry. Journal of Geochemical Exploration, 192: 142–154.

German, C.R., Klinkhammer, G.P., Edmond, J.M., Mura, A., and Elderfield, H., 1990. Hydrothermal scavenging of rare-earth elements in the ocean. Nature, 345(6275): 516–518.

Gieré, R., 1996. Formation of rare earth minerals in hydrothermal systems. Rare Earth Minerals: Chemistry, Origin and Ore Deposits. The Mineralogical Society Series 7: Chapman & Hall, London, 372.

Guizhou Bureau of Geology and Mineral Resources., 1987. Areaal geology of Guizhou Province. Geological Publishing House, 1–698 (in Chinese).

Guo, F., Fan, W.M., Wang, Y.J., and Li, C.W., 2004. When did the Emeishan Mantle Plume activity start? Geochronological and geochemical evidence from Ultramafic-Mafic Dikes in southwestern China. International Geology Review, 46(3): 226–234.

Haas, J.R., Shock, E.L., and Sassani, D.C., 1995. Rare earth elements in hydrothermal systems: estimates of standard partial molar thermodynamic properties of aqueous complexes of the rare earth elements at high pressures and temperatures. Geochimica et Cosmochimica Acta, 59(21): 4329–4350.

Harmon, R.S., and Hoefs, J., 1995. Oxygen isotope heterogeneity of the mantle deduced from global 18O systematics of basalts from different geotectonic settings. Contributions to Mineralogy and Petrology, 120(1): 95–114.

Hein, J.R., and Kosk, R.A., 1987. Bacterially mediated diagenetic origin for chert-hosted manganese deposits in the Franciscan Complex, California Coast Range. Geology, 15(8): 722–726.

Hoefs, J., 1997. Stable Isotope Geochemistry. Springer-Verlag, Berlin, 140.

Hou, Z.L., 1997. The surrounding manganese ore of Yangtze platform. Metallurgical Industry Press, 1–135. (in Chinese)

Hou, Z.Q., Chen, W., and Lu, J.R., 2006. Eruption of the continental flood basalts at -259 Ma in the Emeishan Large Igneous Province, SW China: Evidence from Laser Microprobe 40Ar/39Ar Dating. Acta Geologica Sinica (English edition), 80(4): 514–521.

Huang, H., Du, Y.S., Yang, J.H., Zhou, L., Hu, L.S., Huang, H.W., and Huang, Z.Q., 2014. Origin of Permian basalts and clastic rocks in Napo, Southwest China: Implications for the erosion and eruption of the Emeishan Large Igneous Province. Lithos, 208-209: 324–338.

Huang, Z.L., Jin, Z.G., Xiang, X.L., Gu, J., Wu, G.H., Chen, X.L., Su, Z.L., Zhao, Y.Y., Ye, L., and Zhou, L., 2014. Metallogenic theory and prediction of Bauxite deposits in the Wuchuan-Zhen'an-Daozhen area, northern Guizhou Province, China. Beijing: Science Press, 102–121 (in Chinese).

Kato, Y., Fujinaga, K., Nozaki, T., Osawa, H., Nakamura, K., and Ono, R., 2005a. Rare earth, major and trace elements in the Kunimiyama ferromanganese deposit in the Northern Chichibu belt, Central Shikoku, Japan. Resource Geology, 55 (4): 291–299.

Kato, Y., Fujinaga, K., and Suzuki, K., 2005b. Major and trace element geochemistry and Os isotopic composition of metalliferous umbers from the late Cretaceous Japanese accretionary complex. Geochemistry Geophysics Geosystems, 6(7): 1–20.

Kawabe, I., Kitahara, Y., and Naito, K., 1991. Non-chondritic yttrium/holmium ratio and lanthanide tetrad effect observed in pre-Cenozoic limestones. Geochemical Journal, 25: 31–44.

Lafaye, F.G., and Weber, F., 2003. Natural nuclear fission reactors: time comstraints for occurrence, and their relation to uranium and manganese deposits and to the evolution of the atmosphere. Precambrian Research, 120(1): 81–100.

Liakopoulos, A., Glasby, G.P., Papavassiliou, C.T., and Boulegue, J., 2001. Nature and origin of the Vani manganese deposit, Misos, Greece: an overview. Ore Geology Reviews, 18(3): 181–209.

Li, H.B., Zhang, Z.C., Ernst, R., L, L.S., Santosh, M., Zhang,D.Y., and Cheng, Z.G., 2015. Giant radiating mafic dyke swarm of the Emeishan Large Igneous Province: Identifying the mantle plume centre. Terra Nova, 27(4): 247–257.

Li, H.B., Zhang, Z.C., Santosh, M., L, L.S., Liu, H., and Liu,W., 2017. Late Permian basalts in the Yanghe area, eastern Sichuan Province, SW China: Implications for the geodynamics of the Emeishan flood basalt province and Permian global mass extinction. Journal of Asian Earth Sciences, 134: 293–308.

Liu, P., Liao, Y.C., Yin, K.H., Ye, D.S., Zhu, H., Han, Z.H., and Yang, G.L., 2008. Hydrothermal sedimentary manganese deposits associated to volcanic activities-Permian manganese deposit in Guizhou. Geology in China, 35(5): 992–1006 (in Chinese with English abstract).

Liu, X.F., Wang, Q.S., and Gao, X.J., 1989. Manganese deposits of Guizhou, China: Guiyang. Guizhou people's Press, 7–56 (in Chinese).

Liu, Z.C., Wang, C., Zhang, Y.G., Fang, B., Chen, D., Wei, Z.Q., and Cui, Z.Q., 2015. Geochemistry and ore genesis of Zunyi

manganese deposit, Guizhou Province, China. Acta Mineralogica Sinica, 35(4): 481–488 (in Chinese with English abstract).
Liu, Z.C., Zhang, Y.G., Chen, D., Tie, Y.H., Cui, Z.Q., Hu, L.Y., and Zhong, Y.L., 2013. Geochemical characteristics and geological significance of "Bainitangceng" siliceous rocks in Zunyi manganese ore fields, Guizhou Province, China. Acta Mineralogica Sinica, 33(4): 231–236 (in Chinese with English abstract).
Lo, C.H., Chung, S.L., Lee, T.Y., and Wu, G.Y., 2002. Age of the Emeishan flood magmatism and relations to Permian–Triassic boundary events. Earth and Planetary Science Letters, 198(3–4): 449–458.
Maynard, J.B., 2010. The chemistry of manganese ores throughtime: a signal of increasing diversity of earth-surface environments. Economic Geology, 105(3): 535–552.
Michard, A., 1989. Rare earth element systematics in hydrothermal fluids. Geochimica et Cosmochimica Acta, 53 (3): 745–750.
Mishra, P., Mvohapatra, B.K., and Singh, P.P., 2006. Mode of occurrence and characteristics of manganese-ore bodies in Iron Ore Group of rocks, North Orissa, India and its significance in resource evaluation. Resource Geology, 56(1): 55–64.
Mohapatra, B.K., Paul, D., and Sahoo, R.K., 2006. REE distribution in ferromanganese oxide ores from Iron Ore Group, Western Koira Valley, Orissa, India. Journal of Mineralogy Petrology and Economic Geology, 91(7): 266–274.
Mongelli, G., Mameli, P., Oggiano, G., and Sinisi, R., 2013. Generation of Ce anomalies in SW Sardinian manganese ores. Journal of Geochemical Exploration, 133: 42–49.
Moriyama, T., Panigrahi, M.K., Pandit, D., and Waanabe, Y., 2008. Rare earth element enrichment in Late Archean manganese deposits from the Iron Ore Group, East India. Resource Geology, 58(4): 402–413.
Nozaki, Y., Zhang, J., and Amakawa, H., 1997. The fractionation between Y and Ho in the marine environment. Earth and Planetary Science Letters, 148(1): 329–340.
Nyame, F.K., Beukes, N.J., Kase, K., and Yamamoto, M., 2002. Compositional variations in manganese carbonate micronodules from the Lower Proterozoic Nsuta deposit, Ghana: product of authigenic precipitation or post-formational diagenesis. Sedimentary Geology, 154(3-4): 159–175.
Okita, P.M., Maynard, J.B., Spiker, E.C., and Force, E.R., 1988. Isotopic evidence for organic matter oxidation by manganese reduction in the formation of stratiform manganese carbonate ore. Geochimica et Cosmochimica Acta, 52(11): 2679–2685.
Oksuz, N., 2011. Geochemical characteristics of the Eymir (Sorgun-Yozgat) manganese deposit, Turkey. Journal of Rare Earths, 29(3): 287–296.
Papavassiliou. V. K., Glasby, G., Alfieris, D., Mitsis, I., 2017. New geochemical and mineralogical constraints on the genesis of the Vani hydrothermal Mn deposit at NW Milos island, Greece: Comparison with the Aspro Gialoudi deposit and implications for the formation of the Milos Mn mineralization. Ore Geology Reviews, 80: 594–611.
Pfeifer, H.R., Oberänsli, H., and Epprecht, W., 1988. Geochemical evidence for a synsedimentary hydrothermal origin of Jurassic iron–manganese deposits at Gonzen (Sargans, Helvetic Alps, Switzerland). Marine Geology, 84(3-4): 257–272.
Ramos, Preston PCC., 2001. Physical and chemical characterisation of the manganese ore bed at the Mamatwan mine, Kalahari manganese Field [MSc dissertation]. Johannesburg: Rand Afrikaans University, 101.
Shellnutt, J.G., 2014. The Emeishan large igneous province: A synthesis. Geoscience Frontiers, 5(3): 369–394.
Sinisi, R., Mameli, P., Mongelli, G., and Oggiano, G., 2012. Different Mn-ores in a continental arc setting: geochemical and mineralogical evidences from Tertiary deposits of Sardinia (Italy). Ore Geology Reviews, 47: 110–125.
Sun, S.S., and Mcdonough, W.F., 1989. Chemical and isotopic systematics of oceanic basalts: implications for mantle composition and processes. Geological Society London Special Publications, 42(1): 313–345.
Song, X.Y., Keays, R.R., Xiao, L., Qi, H.W., and Ihlenfeld, C., 2009. Platinum-group element geochemistry of the continental flood basalts in the central Emeishan Large Igneous Province, SW China. Chemical Geology, 262(3-4): 246–261.
Tao, Y., Ma, Y.S., Miao, L.C., and Zhu, F.L., 2009. SHRIMP U-Pb zircon age of the Jinbaoshan ultramafic intrusion, Yunnan Province, SW China. Chinese Science Bulletin, 54(22): 168–172 (in Chinese with English abstract).
Taylor, B.E., 1986. Magmatic volatiles; isotopic variation of C, H, and S. Reviews in Mineralogy and Geochemistry, 16: 185–225.
Taylor, S.R., and Mclennan, S.M., 1985. The continental crust: its composition and evolution. The Journal of Geology, 94(4): 57–72.
Ukstins-Peate, I., and Bryan, S.E., 2008. Re-evaluating plume-induced uplift in the Emeishan Large Igneous Province. Nature Geoscience, 1(9): 625–629.
Vaniman, D.T., Chipera, S.J., Bish, D.L., Duff, M.C., and Hunter, D.B., 2002. Crystal chemistry of clay-manganese oxide associations in soils, fractures, and matrix of the Bandelier Tuff, Pajarito Mesa, New Mexico. Geochim. Cosmochim. Acta, 66(8): 1349–1374.
Wright, J., and Holser, W.T., 1987. Paletedox variations in ancient oceans recorded by rare earth elements in fossil apatite. Geochim. Cosmochim. Acta, 51: 631–644.
Wu, C.Q., Zhang, Z.W., Xiao, J.F., Fu, Y.Z., Shao, S.X., Zheng, C.F., Yao, J.H., and Xiao, C.Y., 2016. Nanhuan manganese deposits within restricted basins of the southeastern Yangtze Platform, China: Constraints from geological and geochemical evidence. Ore Geology Reviews, 75: 76–99.
Xie, J.C., Sun, W.D., Du, J.G., Xu, W., Wu, L.B., Yang, X., and Zhou, T., 2013. Geochemical studies on Permian manganese deposits in Guichi, Eastern China: Implications for their origin and formative environments. Journal of Asian Earth Sciences, 74: 155–166.
Xie, H., and Zhu, L.J., 2012. Existing state and distribution regularity of rare earth elements from early Cambrian phosphorite in Guizhou. Journal of the Chinese Society of Rare Earths, 30(5): 112–119 (in Chinese with English abstract).
Xu, C., Kynický, J., Smith, M.P., Kopriva, A., Brtnický, M., Urubek, T., Yang, Y.S., Zhao, Z., He, C., and Song, W.L., 2017. Origin of heavy rare earth mineralization in South China. Nature Communications, 8: 1–8.
Xu, H., Gao, J.B., Yang, R.D., Zheng, L.L., and Zhang, X., 2017. The origin of siliceous rocks in Zunyi Permian manganese ore fields in Guizhou Province and their metallogenic significance. Chinese Journal of Geology, 52(4): 1297–1311 (in Chinese with English abstract).
Xu, H., Gao, J.B., Yang, R.D., Chen, J., Zhang, X., and Zheng, L.L., 2018. Occurrence of rare earth element in Permian manganese Deposits in Zunyi, Guizhou Province, China. Journal of the Chinese Society of Rare Earths, 36(3): 357–364 (in Chinese with English abstract).
Xu, Y.G., Wang, C.Y., and Shen, S.Z., 2014. Permian Large Igneous Provinces: characteristics, mineralization and paleo-environment effects. Lithos, 204: 1–3.
Yang, R.D., Wang, W., Zhang, X.D., Liu, L., Wei, H.R., Bao, M., and Wang, J.X., 2008. A new type of rare earth elements deposit in weathering crust of Permian basalt in western Guizhou, NW China. Journal of Rare Earths, 26(5): 753–759.
Yang, R.D., Cheng, M.L., and Wei, H.R., 2009. Geochemical characteristics and origin of a manganese deposit in the Middle Permian Maokou formation in Shuicheng, Guizhou, China. Geotectonica and Metallogenia, 33(4): 613–619 (in Chinese with English abstract).
Yang, R.D., Cheng, M.L., Gao, J.B., Xu, H., Li, J., Chen, J., and Liu, K., 2018. The sedimentary characteristic and orgion of manganese deposit in the middle Permian Maokou Formation in Guizhou, China. Acta Geologica Sinica, 92(4): 804–816 (in Chinese with English abstract).
Yeh, H.W., Hein, J.R., Jie, Y., and Fan, D.L., 1999. Stable isotope, chemical, and mineral compositions of the Middle Proterozoic Lijiaying manganese deposit, Shaanxi Province,

China. Ore Geology Reviews, 15(1-3): 55–69.
Yumul, Jr.G.P., Zhou, M.F., Wang, C.Y., Zhou, T.P., and Dimalanta, C.B., 2008. Geology and geochemistry of the Shuanggou ophiolite (Ailao Shan ophiolitic belt), Yunnan Province, SW China: Evidence for a slow-spreading oceanic basin origin. Journal of Asian Earth Sciences, 32(5–6): 385–395.
Zeng, Y.Y., and Liu, T.B., 1999. Characteristics of the Devonian Xialei manganese deposit, Guangxi Zhuang Autonomous region, China. Ore Geology Reviews, 15(1): 153–163.
Zhang, Z.W., Zheng, G.D., Takahashi, Y., Wu, C.Q., Zheng, C.F., Yao, J.H., and Xiao, C.Y., 2016. Extreme enrichment of rare earth elements in hard clay rocks and its potential as a resource. Ore Geology Reviews, 72: 191–212.
Zheng, Y.F., and Chen, J.F., 2000. Geochemistry of Stable Isotope. Beijing: Science publishing, 143–214 (in Chinese).
Zhong, H., and Zhu, W.G., 2006. Geochronology of layered mafic intrusions from the Pan–Xi area in the Emeishan Large Igneous Province, SW China. Mineralium Deposita, 41(6): 599–606.
Zhong, Y.T., He, B., Mundil, R., and Xu, Y.G., 2014. CA-TIMS zircon U–Pb dating of felsic ignimbrite from the Binchuan section: Implications for the termination age of Emeishan Large Igneous Province. Lithos, 204: 14–19.
Zhou, L.J., Zhang, Z.W., Li, Y.J., You, F.H., Wu, C.Q. and Zheng, C.F., 2013. Geological and geochemical characteristics in the paleo-weathering crust sedimentary type REE deposits, western Guizhou, China. Journal of Asian Earth Sciences, 73 (5): 184–198.
Zhou, M.F., Malpas, J., Song, X.Y., Robinson, P.T., Sun, M., Kennedy, A.K., Lesher, C.M., and Keays, R.R., 2002. A temporal link between the Emeishan Large Igneous Province (SW China) and the end-Guadalupian mass extinction. Earth and Planetary Science Letters, 196(3–4): 113–122.
Zhou, M.F., Zhao, J.H., Qi, L., Su, W.C., and Hu, R.Z., 2006. Zircon U-Pb geochronology and elemental and Sr–Nd isotope geochemistry of Permian mafic rocks in the Funing area, SW China. Contributions to Mineralogy and Petrology, 151(1): 1–19.
Zhu, J., Zhang, Z.C., Hou, T., and Kang, J.L., 2011. LA-ICP-MS zircon U-Pb geochronology of the tuffs on the uppermost of the Emeishan basalt succession in Panxian County, Guizhou Province: Constraints on genetic link between Emeishan Large Igneous Province and the mass extinction. Acta Petrologica Sinica, 27(9): 2743–2751 (in Chinese with English abstract).

About the first author



XU Hai, male, born in 1993 in Tongren City, Guizhou Province; Ph.D.; College of Resources and Environmental Engineering, Guizhou University, Guiyang, China; Engages in the study of mineral deposits and geochemistry. Email: xuhai803@163.com; Phone: 18184160286.

About the corresponding author



GAO Junbo, male, born in 1985, native of Weinan, Shanxi Province; Doctor, associate professor of the Department of Earth Science of Guizhou University; Master's tutor; Engaged in geological environment and sedimentary deposit teaching and research. Email: gaojunbo1985@126.com; Phone: 18785196708.